LBL-21995
Preprint

Lawrence Berkeley Laboratory
UNIVERSITY OF CALIFORNIA

Materials & Chemical Sciences Division

Submitted to Physical Review A

A COMPLETE PHOTOEMISSION STUDY OF THE He $1s^2 \rightarrow 3s3p$ AUTOIONIZING RESONANCE

D.W. Lindle, T.A. Ferrett,
P.A. Heimann, and D.A. Shirley

March 1987

Prepared for the U.S. Department of Energy under Contract DE-AC03-76SF00098

DISCLAIMER

LBL-21995

A COMPLETE PHOTOEMISSION STUDY OF THE He $1s^2 \rightarrow 3s3p$ AUTOIONIZING RESONANCE

D.W. Lindle, T.A. Ferrett, P.A. Heimann, and D.A. Shirley

Materials and Chemical Sciences Division
Lawrence Berkeley Laboratory
and
Department of Chemistry
University of California
Berkeley, California 94720

This work was supported by the U.S. Department of Energy under Contract No. DE-AC03-76SF00098.

LBL-21995

A COMPLETE PHOTOEMISSION STUDY OF THE He $1s^2 \rightarrow 3s3p$ AUTOIONIZING RESONANCE

D.W. Lindle,* T.A. Ferrett,* P.A. Heimann,† and D.A. Shirley

Materials and Chemical Sciences Division
Lawrence Berkeley Laboratory
and
Department of Chemistry
University of California
Berkeley, California 94720

The total absorption cross section of He and the $He^+(1s)$ partial cross section have been measured using photoelectron spectroscopy and synchrotron radiation in the photon-energy region of the $1s^2 \rightarrow 3s3p$ resonance. The effects of autoionization are relatively small, causing deviations of 5-10% from the nonresonant cross sections. These new measurements, along with a previous study of the 3s3p resonance behavior of the $He^+(n=2)$ satellite cross section, branching ratio, and angular-distribution parameter, allow the complete determination of all the parameters governing the $1s^2 \rightarrow 3s3p$ resonance. From these experimentally determined parameters, we have derived all of the relevant oscillator strengths and individual dipole and Coulomb matrix elements which describe He photoionization in the vicinity of the 3s3p doubly excited state.

---

*Present address: National Bureau of Standards, Gaithersburg, MD 20899.
†Present address: Physik-Department E20, Technische Universität München, 8046 Garching b. München, W. Germany.

I. Introduction

The photoionization of helium provides the simplest example of electron correlation in atomic physics. For this reason, much recent work[1-26] has been performed on the near-threshold behavior of the $He^+(n\ell)$ correlation satellites. Particular attention has been directed to the $He^+(n=2)$ satellite,[1-12,14-26] which contains the effectively degenerate $He^+(2s)$ and $He^+(2p)$ final states. The available experimental results include measurements of the $He^+(n=2)$ satellite cross section,[1-5,12] its branching ratio relative to the 1s main line,[1-8,11] its angular-distribution asymmetry parameter,[6,7,9-12] and the cross-section ratio for photoionization to the 2p final state relative to the 2s final state.[6-12] These results have been combined successfully with theoretical calculations[16-26] to increase our understanding of the effects of continuum-state electron correlation.

A different perspective on electron correlation is provided by studying the effects of autoionization on the photoemission processes leading to satellite final states.[8,11,24,26] In He, the first autoionization resonance which lies above a satellite threshold is the 3s3p doubly excited state. Photoemission decay from this state can yield energetically only $He^+(1s)$ or $He^+(n=2)$, making this excitation relatively easy to study. A previous paper[11] (which we shall refer to as I), determined the behavior of the n=2 cross section, branching ratio, and photoelectron asymmetry parameter near the 3s3p resonance. Also presented in I were qualitative results for the total cross

section (determined from electron-yield measurements) and the 1s main-line partial cross section at this resonance. All of these were combined to derive a few of the oscillator strengths and matrix elements which govern the 3s3p autoionization process.

In this work, we extend the experimental results in I by presenting the quantitative resonance profiles for the He total cross section σ_T and the 1s partial cross section σ_{1s} in the vicinity of the 3s3p resonance. The new measurements indicate only small relative effects (5-10%) on these cross sections on resonance, but both Fano-type profiles exhibit some asymmetry. The magnitude of the resonant oscillation in the total cross section is found to be larger by a factor of 5 than an earlier photoabsorption measurement,[27] but it agrees with other photoemission results,[10] including the qualitative behavior discerned in I. With the availability of these new quantitative measurements for σ_T and σ_{1s}, as well as the n=2 results in I, we present a detailed derivation of all the oscillator strengths and individual dipole and Coulomb matrix elements which describe autoionization of the 3s3p resonance. These results are obtained with minimal dependence on theoretical values or simplifying assumptions. This complete set of information about the 3s3p resonance thus may provide a starting point for detailed theoretical interpretations of the electron-correlation phenomena that are important both to the production of the n=2 satellite and to the autoionization process. This may be particularly useful because He can be considered as a test case in the study of continuum state electron-electron interactions.

The experimental procedures are described in Sec. II, the results are discussed in Sec. III, and conclusions are presented in Sec. IV.

II. Experimental

The experiment was performed at the Stanford Synchrotron Radiation Laboratory, with the same apparatus[28] and experimental conditions as described in I, with one exception. In the present work, we accepted a slightly poorer photon resolution of 0.19 eV (0.48 Å) full-width at half maximum (FWHM), compared to 0.17 eV (0.43 Å) in I.

The angular distribution of photoelectrons ejected from a randomly oriented sample by linearly polarized radiation, in the dipole approximation, is given by

$$\frac{d\sigma(h\nu,\theta)}{d\Omega} = \frac{\sigma(h\nu)}{4\pi} [1 + \beta(h\nu)P_2(\cos\theta)] , \quad (1)$$

where $h\nu$ is the photon energy, θ is the angle between the propagation vector of the photoelectron and the polarization vector of the ionizing radiation, $\sigma(h\nu)$ is the cross section, $\beta(h\nu)$ is the asymmetry parameter that completely describes the angular distribution, and $P_2(\cos\theta)$ is the second Legendre polynomial. The 1s main-line and n=2 intensities were obtained with a single time-of-flight electron analyzer placed at the magic angle [θ=54.7°, for which $P_2(\cos\theta)$=0], thereby eliminating any angular dependence of the photoelectron peak intensities. The relative total cross section then

was determined by summing the two measured peak intensities (1s and n=2) at each photon energy.

III. Results and Discussion

The analysis and interpretation of the measurements presented in this section draw heavily on the resonance photoionization discussion in I.[11] Therefore, the organization of this section follows closely that of Sec. IV of I, and several of the equations and explanations common to both works are omitted here. The reader is referred to the previous publication[11] for further information and discussion.

The remainder of this section will deal with analysis of the total cross section and the 1s and n=2 partial cross sections for He over the 3s3p resonance. To lay the groundwork for this analysis, we begin in Sec. IIIA with a review of the Fano and Starace formalisms that are used to describe the observed autoionization phenomena. The methods used to fit the data with these formalisms are discussed in Sec. IIIB. In Sec. IIIC, we present the quantitative results for σ_T and σ_{1s}, and the parameters used to describe the autoionization profiles. From the resonance parameters, the α_μ parameters of Starace are derived in Sec IIID. Finally, Sec. IIIE illustrates the determination of oscillator strengths and matrix elements, which together provide a complete description of the $1s^2 \rightarrow 3s3p$ autoionizing resonance.

A. Theoretical Background

The effect of an isolated resonance, such as a Rydberg level, on the total photoabsorption or total photoionization cross section was derived originally by Fano.[29] The presence of a discrete level embedded in one or more continua causes an interference in the photon absorption process because of the indistinguishability of the two pathways, direct ionization and autoionization, leading to the final state. Fano derived the following expression for the total cross section σ_T for the case of an isolated discrete state interacting with one or more continuum states:

$$\sigma_t = \sigma_0 \left[\rho^2 \frac{(q + \epsilon)^2}{1 + \epsilon^2} + 1 - \rho^2 \right], \tag{2a}$$

$$\epsilon = \frac{E - E_0}{\Gamma/2}, \tag{2b}$$

where the Fano parameters q and ρ^2 are assumed constant over the resonance, σ_0 is the nonresonant cross section, Γ and E_0 are the linewidth (FWHM) and the energy of the resonance, respectively, and ϵ is a reduced energy.

The quantities q, ρ^2, σ_0 and Γ can be expressed in terms of the dipole matrix elements for transitions from the ground state g to the discrete state ϕ, and to the continua μ, together with the Coulomb-interaction matrix elements coupling the discrete state to the continua. The q parameter, which governs the shape of the total cross

section, is given by

$$q = \frac{\langle \Phi | \vec{r} | g \rangle}{\pi \sum_{\mu} \langle \phi | V | \mu \rangle \langle \mu | \vec{r} | g \rangle} , \tag{3}$$

and the correlation coefficient ρ^2, which is a measure of the strength of the resonance, is given by

$$\rho^2 = \frac{\sum_{\mu} |\langle \phi | V | \mu \rangle \langle \mu | \vec{r} | g \rangle|^2}{\sum_{\mu} |\langle \phi | V | \mu \rangle|^2 \sum_{\mu} \langle \mu | \vec{r} | g \rangle|^2} , \tag{4}$$

where $\vec{r}$ and V represent the dipole and Coulomb operators, respectively, and Φ is the discrete state modified by an admixture of the continuum states. The degree to which Φ is different from ϕ is dependent upon the energy variations of the continuum wavefunctions in the vicinity of the resonance. The linewidth of the resonance is given by

$$\Gamma = 2\pi \sum_{\mu} |\langle \phi | V | \mu \rangle|^2 , \tag{5}$$

and the nonresonant, background cross section is given by

$$\sigma_0 = \sum_{\mu} |\langle \mu | \vec{r} | g \rangle|^2 . \tag{6}$$

While the matrix elements in Eqs. (3) and (4) are not strictly energy-independent, they are slowly-varying functions of energy; therefore q and ρ^2 are assumed to be constant in the vicinity of a resonance.

The Fano parametrization [Eqs. (2)-(6)] was derived to explain the behavior of the total absorption cross section in the vicinity of an isolated resonance. In a photoemission experiment, however, partial cross sections are measured. Although the functional form of Eq (2) clearly is appropriate for describing the shape of the resonance profile for a partial cross section, the representation of the resonance behavior of a partial cross section in terms of the dipole and Coulomb matrix elements is not given by Eqs. (2)-(6). Starace[30] has addressed the problem of several outgoing channels in the vicinity of an autoionization resonance. Davis and Feldkamp[31] and Combet-Farnoux[32] have derived equivalent expressions. We shall use the notation of Starace. His expression for the partial cross section for each of the observable photoemission channels μ is

$$\sigma(\mu) = \frac{\sigma_0(\mu)}{1+\epsilon^2}\left\{\epsilon^2 + 2[q\mathrm{Re}(\alpha_\mu) - \mathrm{Im}(\alpha_\mu)]\epsilon + 1 - 2q\mathrm{Im}(\alpha_\mu) - 2\mathrm{Re}(\alpha_\mu) + (q^2+1)|\alpha_\mu|^2\right\}, \quad (7)$$

where $\sigma_0(\mu)$ is the nonresonant partial cross section for the μth observable final state, and ϵ and q are defined in Eqs. (2b) and (3), respectively. The complex parameter α_μ is given by[33]

$$\alpha_\mu = \frac{\langle\phi|V|\mu\rangle}{\langle g|\vec{r}|\mu\rangle}\left[\frac{2\pi}{\Gamma}\sum_\mu \langle g|\vec{r}|\mu\rangle\langle\mu|V|\phi\rangle\right], \quad (8)$$

with Γ given by Eq. (5). The term in brackets is common to all channels. The squares of the α_μ parameters can be thought of as

replacing ρ^2 as the correlation coefficient for each channel when partial cross sections are measured. It is important to note that each μ represents an observable photoionization channel [eg. $He^+(1s\varepsilon p)$]. This restriction was not necessary in the Fano derivation of the resonance behavior of the total cross section, because the individual photoemission channels only appeared in summations over μ.

It is clear that the Fano and Starace parametrizations for the total cross section and partial cross sections can be expressed in the same mathematical form[30-32] as follows;

$$\sigma_t = \sigma_0 \left[\frac{C_1 + C_2\epsilon + \epsilon^2}{1 + \epsilon^2} \right], \tag{9}$$

where C_1 and C_2 can be given in terms of either q and ρ^2 or α_μ. Equation (9) describes the characteristic behavior of a cross section in the vicinity of an autoionization resonance. We will refer to q and ρ^2 as the Fano parameters, and $C_1(\mu)$ and $C_2(\mu)$ given by Eq. (7) as the Starace parameters. Further discussion of these formalisms may be found in I.

Finally, an additional complication is that the n=2 satellite peak actually contains three photoemission channels μ: $2s\varepsilon p$, $2p\varepsilon s$, and $2p\varepsilon d$. Thus, the partial cross section for the n=2 photoelectron peak $\sigma(n=2)$ is the sum of three $\sigma(\mu)$. The expression for $\sigma(n=2)$ is of the same form as Eq. (7), but with $\sigma_0(\mu)$ replaced by the off-resonance partial cross section for the unresolved channels $\sigma_0(n=2)$, and $Re(\alpha_\mu)$, $Im(\alpha_\mu)$, and $|\alpha_\mu|^2$ replaced by $Re\langle\alpha\rangle_{n=2}$, $Im\langle\alpha\rangle_{n=2}$,

and $\langle|\alpha|^2\rangle_{n=2}$, which are averaged quantities weighted by the $\sigma_0(\mu)$. This complication also was discussed in Ref. 34 and in I for the case of spin-orbit split continuum states, such as $1s\epsilon p_{1/2}$ and $1s\epsilon p_{3/2}$, which contribute to the same photoelectron peak. However, this latter effect is ignored in the present work, as it was for most of the analysis presented in I.

B. Data Analysis

This work presents the resonance behavior of the He total cross section and the $He^+(1s)$ photoemission cross section in the photon-energy region of the $1s^2 \rightarrow 3s3p$ resonance. The behavior of the $He^+(n=2)$ satellite over this resonance was given in I. The total cross section and the 1s partial cross section are displayed in Table I and in Figs. 1 and 2, respectively. The data were normalized to the absorption values given by Marr and West[35] at 68.9 eV, as was done in I.

The σ_T data in Fig. 1 were fitted to the Fano formula, Eq. (2), convoluted with a Gaussian function of 0.19 eV (0.48 Å) FWHM to account for monochromator broadening. The nonresonant cross section σ_0 was taken to be a linear function of the photon energy E throughout the resonance region. The 3s3p resonance position and width were taken from Woodruff and Samson to be 69.917 eV and 0.178 eV, respectively.[8] The Fano parameters for the best fit are presented in Table II, and the solid curve in Fig. 1 illustrates the resulting fit.

The Fano formula also was used to fit σ_{1s} over the 3s3p resonance, in a manner identical to that for σ_T. Once the Fano parameters for σ_{1s} were obtained, Eqs. (2) and (9) were used to determine the 1s Starace parameters, which are the most easily interpreted parameters for a partial-cross-section measurement. The results for σ_{1s} are given in Table III.

C. Resonance Parameters

The Fano parameters determined from the fits to σ_T and σ_{1s} over the 3s3p resonance are listed in Tables II and III, respectively. The corresponding values for $\sigma_{n=2}$ from I also are given in Table III. For the partial cross sections, σ_{1s} and $\sigma_{n=2}$, we show in Table III the Starace parameters C_1 and C_2. The values for $\sigma_{n=2}$ are in good agreement with those of Woodruff and Samson,[8] as discussed in I. The present results for σ_{1s} are in agreement with another photoemission experiment,[10] but disagree somewhat with the numbers given in I, which were obtained from a qualitative analysis of the resonance profiles.

For σ_T, the values presented here disagree with both the qualitative analysis of I and the absorption results of Dhez and Ederer.[27] However, the present results in Figs. 1 and 2 and the $\sigma_{n=2}$ results from I do confirm the conjecture made in I that the profiles of σ_T, σ_{1s}, and $\sigma_{n=2}$ all have the same "phase" over the 3s3p resonance. By the same phase, we refer to the fact that the resonance cross-section minima all occur on the low-energy side of the

resonance (i.e. the Fano q parameter is positive for all three cross sections). We note that although the ρ^2 parameter for σ_T from Ref. 27 is too small by a factor of 5, the q parameter from this earlier experiment agrees well with the present result. The discrepancy in ρ^2 possibly is a result of saturation effects in the photoabsorption measurement (Ref. 27).

The values of q and ρ^2 for σ_T also can be compared to theoretical determinations of the resonance parameters. Fano and Cooper[36] estimated q and ρ^2 to be 1.7 and 0.01, respectively. Calculations by Senashenko and Wagué[37] using the diagonalization approximation yielded q = 1.31 and ρ^2 = 0.019. Both of these determinations disagree with the larger value of ρ^2 measured here, but agree with the value of q.

Comparing now the magnitudes of ρ^2 for the total and partial cross sections in Tables II and III, we see that it is small for σ_T and σ_{1s}, but very large for $\sigma_{n=2}$. This observation is borne out in Figs. 1 and 2 in that the relative effect on σ_T and σ_{1s} is less than 10% in both cases. The results for $\sigma_{n=2}$ in I and Ref. 8, on the other hand, indicate an effect of nearly 100% for this partial cross section.

D. α_μ Parameters

This subsection will illustrate the quantitative methods for extracting the α_μ parameters from the measured results for σ_T,

σ_{1s}, and $\sigma_{n=2}$ contained in Tables II and III. In I, we determined only the α_μ parameters for the 1s and combined n=2 (2sεp, 2pεs, and 2pεd) photoemission peaks. With the more quantitative results in this work, we are able to derive, with minimal assumptions, meaningful values for the α_μ parameters for the individual channels which constitute the n=2 satellite peak. Also derived in this subsection are partial linewidths, which provide additional measures, besides the $|\alpha_\mu|^2$, of the strength of the resonance effect for each photoemission channel.

We begin the determination of the α_μ parameters by recognizing that Eqs. (7) and (9) can be combined to yield expressions for the Starace parameters, C_1 and C_2, in terms of $\mathrm{Re}(\alpha_\mu)$, $\mathrm{Im}(\alpha_\mu)$, $|\alpha_\mu|^2$, and the Fano q parameter for the total cross section. For $He^+(1s)$, the three α_μ parameters are related by

$$[\mathrm{Re}(\alpha_{1s})]^2 + [\mathrm{Im}(\alpha_{1s})]^2 = |\alpha_{1s}|^2 \quad , \tag{10}$$

Thus, we have three equations in three unknowns, which yield a quadratic equation for $\mathrm{Re}(\alpha_{1s})$. The solution is given in Table IV, along with the concomitant results for $\mathrm{Im}(\alpha_{1s})$ and $|\alpha_{1s}|^2$.

Using the value of $|\alpha_{1s}|^2$ and the sum rule for $|\alpha_\mu|^2$ parameters given in Ref. 33, we determine $\langle|\alpha|^2\rangle_{n=2}$, where the brackets signify that this is an averaged quantity over the three photoemission channels contributing to the n=2 satellite peak. Having derived $\langle|\alpha|^2\rangle_{n=2}$, the n=2 Starace parameters in Table III can be used to find $\mathrm{Re}\langle\alpha\rangle_{n=2}$ and $\mathrm{Im}\langle\alpha\rangle_{n=2}$. These values for the n=2 satellite are presented in Table IV.

It is possible to break up the $\alpha_{n=2}$ parameters into their components for the individual channels, $2s\epsilon p$, $2p\epsilon s$, and $2p\epsilon d$. The first step in this derivation is to determine how the n=2 nonresonant cross section $\sigma_0(n=2)$ can be broken into the nonresonant cross sections $\sigma_0(\mu)$ for the three contributing channels. We can do this by considering Fig. 5 of I for the cross-section ratio $R=\sigma_0(2p)/\sigma_0(2s)$. At 69.9 eV, experiment shows the ratio to be 2.2(3), yielding $\sigma_0(2s)$ of 0.030(4) Mb. The remaining n=2 intensity at $h\nu$=69.9 eV [0.067(10) Mb] is divided between the $2p\epsilon s$ and $2p\epsilon d$ channels, but their ratio has been determined experimentally at just two photon energies (65.5 eV and 66.5 eV) closer to the n=2 threshold.[14] However, Ojha[23] has performed a calculation which accurately predicts $\sigma_0(2s)$, R, and $\sigma_0(2p\epsilon s)/\sigma_0(2p\epsilon d)$ as a function of photon energy near the n=2 threshold. Thus, we can use with some confidence Ojha's result for $\sigma_0(2p\epsilon s)/\sigma_0(2p\epsilon d)$, which he found to be 2.0 at 69.9 eV. We have used this theoretical branching ratio to determine $\sigma_0(\mu)$ for the 2p channels. All of the nonresonant cross-section results are shown in Table III.

The averaged parameters $\mathrm{Re}\langle\alpha\rangle_{n=2}$, $\mathrm{Im}\langle\alpha\rangle_{n=2}$, and $\langle|\alpha|^2\rangle_{n=2}$ can now each be broken into three components by assuming a relationship between the 2s and 2p Starace parameters. We can ascertain upper and lower limits on this relationship in the following manner. Recalling the asymmetry-parameter results for the n=2 satellite over the 3s3p resonance given in Fig. 8 of I, we can infer (as described in detail in I) that σ_{2s} and σ_{2p} have the same phase and are very similar in shape to $\sigma_{n=2}$ over the 3s3p resonance.

Furthermore, it was inferred that the ratio R also has the same phase as the partial cross sections, which was interpreted in I to mean that σ_{2p} must reach its cross-section minimum at a slightly lower energy than σ_{2s}. This implies that the Starace parameters $C_1(2p)$ and $C_2(2p)$ are slightly larger than $C_1(2s)$ and $C_2(2s)$, respectively. Thus, the upper limit on the 2s Starace parameters for the 3s3p resonance is $C_n(2s) \leq C_n(2p)$.

To ascertain the lower limit for the 2s Starace parameters, we first recognize that they cannot be much smaller than the 2p parameters, because that would cause σ_{2s} and σ_{2p} to reach their cross-section minima at significantly different energies. We know that the minima must be close in energy because the sum of σ_{2s} and σ_{2p} (i.e. $\sigma_{n=2}$) effectively goes to zero at a particular photon energy.[8] By considering the available $\sigma_{n=2}$ data,[8,11] we estimate that this energy difference is approximately no larger than 0.05 eV. This maximum energy separation of the 2s and 2p cross-section minima yields $C_1(2s) \geq C_1(2p) - 0.5$ and $C_2(2s) \geq C_2(2p) - 1.0$, where we have assumed ρ^2 is the same for σ_{2s} and σ_{2p}.

We can now substitute these upper and lower limits into the following expression;

$$C_n(n=2) = \frac{\sigma_0(2s)}{\sigma_0(n=2)} C_n(2s) + \frac{\sigma_0(2p)}{\sigma_0(n=2)} C_n(2p) \quad , \tag{11}$$

where $C_n(2p)$ represents an average value for the $2p\varepsilon s$ and $2p\varepsilon d$ channels. From Eq. 11, we obtain the allowed ranges of the 2s and 2p Starace parameters. The median values, with error limits extending over the entire allowed ranges, are shown in Table III.

The Starace parameters for σ_{2s} can be treated identically to those for σ_{1s} as described above. In this way, we obtain $Re(\alpha_{2s})$, $Im(\alpha_{2s})$, and $|\alpha_{2s}|^2$, which are presented in Table IV.

Having determined $|\alpha_{2s}|^2$, we can again use the $|\alpha_\mu|^2$ sum rule from Ref. 33 to find $\langle|\alpha|^2\rangle_{2p}$. From this value, it is easy to determine $Re\langle\alpha\rangle_{2p}$ and $Im\langle\alpha\rangle_{2p}$ using the 2p Starace parameters. We cannot derive the α_μ parameters for the individual $2p\epsilon s$ and $2p\epsilon d$ channels. However, because all three of the channels contributing to $\sigma_{n=2}$ go to zero at about the same energy, the Starace parameters for $2p\epsilon s$ and $2p\epsilon d$ can be considered equal to within the errors we have ascribed to them.

The complete set of α_μ parameters derived in this subsection are presented in Table IV. From Eqs. (15) and (16) in Ref. 34 we can determine the partial linewidths Γ_μ for each final state. They are included in Table IV. A check of the α_μ parameters using sum rules for $Re(\alpha_\mu)$ and $Im(\alpha_\mu)$ can be made as described in Ref. 34. The results in Table IV satisfy this check to within the statistical errors, suggesting that no major systematic errors are present in the data analysis.

Table IV contains two measures of the strength of the resonance effect on the photoemission channels. The first measure is $|\alpha_\mu|^2$. We observe that $|\alpha_{1s}|^2$ is two orders of magnitude smaller than the corresponding values for the 2s and 2p channels. This indicates that the resonance effect on the 1s continuum not only produces a small cross-section enhancement (see Fig. 2), but also that configuration interaction of the 3s3p discrete state with the 1s

continuum state is very small. The opposite is true for the 2s and 2p photoemission channels, and thus we observe a large cross-section oscillation in $\sigma_{n=2}$. The second measure of resonance strength is Γ_μ/Γ, with which we again see the dominance of the n=2 channels in the interaction with the excited state. The partial linewidth for the 2s channel is significantly smaller than the sum of the partial linewidths for the 2p channels, even though the $\sigma_0(2p)/\sigma_0(2s)$ cross-section ratio is only 2.2(3) at the resonance energy. This may indicate that the 2p channels, and especially $2p\epsilon s$, couple more strongly to the 3s3p resonance.

The observation that σ_T, σ_{1s}, and $\sigma_{n=2}$ all have the same "phase" over the 3s3p resonance is borne out in the numerical results. The combination of parameters $qRe(\alpha_\mu)-Im(\alpha_\mu)$ $[=C_2(\mu)]$ is greater than zero for all of the channels. The sign of this value directly determines the phase of a partial-cross-section profile. Finally, it appears from the values of $Im(\alpha_\mu)$ in Table IV that the α_μ parameters for the n=2 channels are truly complex. This is expected based on theoretical work[32] which indicates that strong continuum coupling, such as occurs with the 2s and 2p photoemission channels in He, will probably induce the α_μ parameters to be complex.

E. Matrix Elements and Oscillator Strengths

In the previous subsections, we have progressed from the measured data to the resonance parameters to the Starace parameters and partial linewidths for the photoemission channels in the vicinity of the

$1s^2 \rightarrow 3s3p$ resonance in He. Because of the relative simplicity of the He system, it is possible to take one further step and determine the squares of the dipole and Coulomb matrix elements which govern the autoionization process. In this subsection, we will begin with a derivation of the dipole matrix elements, both for the discrete $1s^2 \rightarrow 3s3p$ excitation and for direct ionization. All of these results also will be presented as oscillator strengths. Finally, using the parameters derived in the previous subsection, we will illustrate the determination of the Coulomb matrix elements which are a measure of the coupling of the 3s3p excited state to the available continuum channels.

The oscillator strength f for discrete excitation to the 3s3p resonance can be obtained from the Fano parameters for the total cross section. It is given by[38]

$$f = (0.195\ \mathrm{Ry}^{-1}\mathrm{Mb}^{-1})\ q^2\rho^2\ \sigma_0\ \Gamma\ , \tag{12}$$

with Γ expressed in Rydbergs and σ_0 in Mb. Using the values in Table I, we find $f = 2.4(3) \times 10^{-4}$, which can be compared with the previous estimate[36] of 1.2×10^{-4}. A similar, but possibly more descriptive, expression for f is obtained[39] by replacing q^2 in Eq. (12) with $(q^2 - 1)$. The result for this case is $1.0(3) \times 10^{-4}$. The latter value of f includes the spectral repulsion part of the autoionization profile,[38] and can be considered as the integral of $(\sigma_T - \sigma_0)$ in the vicinity of the 3s3p resonance. Therefore, the use of $(q^2 - 1)$ in Eq. (12) measures the <u>net</u> deviation from the nonresonant background cross section due to the autoionization

resonance. A third expression for f, in which q^2 in Eq. (12) is replaced by $(q^2 + 1)$, measures the <u>total</u> deviation from the background cross section. This last value for f is $3.8(3) \times 10^{-4}$, and possibly is the best result for comparison to other resonances which have profiles that are strictly Lorentzian (i.e. no spectral repulsion).

The dipole matrix element for the $1s^2 \rightarrow 3s3p$ discrete excitation can be determined from Eq. (12).[36] This result and the corresponding oscillator strength from Eq. (12) are given in Table V, along with an estimate made by Fano and Cooper.[36]

The dipole matrix elements describing continuum ionization into the He photoemission channels μ, $|\langle\mu|\vec{r}|1s^2\rangle|^2$, can be determined from σ_0 in Table III for each channel. These values, and their corresponding oscillator strengths, are shown in Table V. In contrast to the values presented in I, we are not multiplying by $(2m_j + 1)$.

The Coulomb matrix elements $|\langle 3s3p|V|\mu\rangle|^2$ can be obtained from Eq. (5) for the partial linewidths derived above. These results also are given in Table V, along with an estimate by Fano and Cooper[36] for the $1s\varepsilon p$ channel.

The matrix elements for the $1s\varepsilon p$ channel derived here agree well with those from I, and also with the estimates made by Fano and Cooper.[36] The continuum dipole matrix elements, which are representative of the nonresonant cross sections, reflect the relationships among the observed cross sections for the 1s, 2s, and 2p photoemission channels. The Coulomb matrix elements, on the other hand, provide a more direct indication of the resonance interactions

in the continuum channels. Here, we see that the $2p\varepsilon s$ configuration seems to be most important in coupling to the discrete state, and that $1s\varepsilon p$, which exhibits a small resonant enhancement, is least important.

IV. Conclusions

The total cross section and the 1s partial cross section in the vicinity of the $1s^2 \rightarrow 3s3p$ autoionizing resonance have been measured. Both resonant profiles show relatively small effects, although the observed oscillation in the total cross section is five times larger than that exhibited in an earlier photoabsorption measurement. Parameters describing the resonance profiles were extracted from the data, and used in conjunction with theory to determine the magnitudes of all of the dipole and Coulomb matrix elements which influence ionization of the He atom in the region of the 3s3p doubly excited state. It is hoped that these individual matrix elements derived from experiment may prove helpful as guides to determining approximate wavefunctions and other parameters for theoretical description of the electron-correlation phenomena that are important to the He system.

Acknowledgements

The authors gratefully acknowledge helpful discussions with A.F. Starace. This work was supported by the Director, Office of Energy Research, Office of Basic Energy Sciences, Chemical Sciences Division of the U.S. Department of Energy under Contract No. DE-AC03-76SF00098. It was performed at the Stanford Synchrotron Radiation Laboratory, which is supported by the Department of Energy's Office of Basic Energy Sciences.

References

1. T.A. Carlson, Phys. Rev. 156, 142 (1967).
2. J.A.R. Samson, Phys. Rev. Lett. 22, 693 (1969).
3. T.A. Carlson, M.O. Krause, and W.E. Moddeman, J. Phys. 32, C4-76 (1971).
4. M.O. Krause and F. Wuilleumier, J. Phys. B 5, L143 (1972).
5. P.R. Woodruff and J.A.R. Samson, Phys. Rev. Lett. 45, 110 (1980).
6. F. Wuilleumier, M.Y. Adam, N. Sandner, and V. Schmidt, J. Physique-Lett. 41, L373 (1980).
7. J.M. Bizau, F. Wuilleumier, P Dhez, D.L. Ederer, T.N. Chang, S. Krummacher, and V. Schmidt, Phys. Rev. Lett. 48, 588 (1982).
8. P.R. Woodruff and J.A.R. Samson, Phys. Rev. A 25, 848 (1982).
9. V. Schmidt, H. Derenbach, and R. Malutzki, J. Phys. B 15, L523 (1982).
10. P. Morin, M.Y. Adam, I. Nenner, J. Delwiche, M.J. Hubin-Franskin, and P. Lablanquie, Nucl. Instrum. Methods 208, 761 (1983).
11. D.W. Lindle, T.A. Ferrett, U. Becker, P.H. Kobrin, C.M. Truesdale, H.G. Kerkhoff, and D.A. Shirley, Phys. Rev. A 31, 714 (1985).
12. P.A. Heimann, U. Becker, H.G. Kerkhoff, B. Langer, D. Szostak, R. Wehlitz, D.W. Lindle, T.A. Ferrett, and D.A. Shirley, Phys. Rev. A 34, 3782 (1986).
13. D.W. Lindle, P.A. Heimann, T.A. Ferrett, and D.A. Shirley, Phys. Rev. A 35, xxxx (1987).
14. J. Jiménez-Mier, C.D. Caldwell, and D.L. Ederer, Phys. Rev. Lett. 57, 2260 (1986).

15. J.M. Bizau, F.J. Wuilleumier, D.L. Ederer, P. Dhez, S. Krummacher, and V. Schmidt (unpublished).

16. E.E. Salpeter and M.H. Zaidi, Phys. Rev. 125, 248 (1962).

17. V. Jacobs, Phys. Rev. A 3, 289 (1971).

18. V.L. Jacobs and P.G. Burke, J. Phys. B 5, L67 (1972).

19. T.N. Chang, J. Phys. B 13, L551 (1980).

20. J.A. Richards, Honours Thesis, Monash University, Australia (1981).

21. K.A. Berrington, P.G. Burke, W.C. Fon, and K.T. Taylor, J. Phys. B 15, L603 (1982).

22. J.A. Richards and F.P. Larkins, J. Electron Spectrosc. 32, 193 (1983).

23. P.C. Ojha, J. Phys. B 17, 1807 (1984).

24. S. Salomonson, S.L. Carter, and H.P. Kelly, J. Phys. B 18, L149 (1985).

25. Y. Kamninos and C.A. Nicolaides, Phys. Rev. A 34, 1995 (1986).

26. S. Salomonson, S.L. Carter, and H.P. Kelly (unpublished results).

27. P. Dhez and D.L. Ederer, J. Phys. B 6, L59 (1973).

28. M.G. White, R.A. Rosenberg, G. Gabor, E.D. Poliakoff, G. Thornton, S.H. Southworth, and D.A. Shirley, Rev. Sci. Instr. 50, 1268 (1979).

29. U. Fano, Phys. Rev. 124, 1866 (1961).

30. A.F. Starace, Phys. Rev. A 16, 231 (1977).

31. L.C. Davis and L.A. Feldkamp, Phys. Rev. B 15, 2961 (1977); 23, 6239 (1981).

32. F. Combet-Farnoux, Phys. Rev. A 25, 287 (1982).

33. P.C. Kemeny, J.A.R. Samson, and A.F. Starace, J. Phys. B 10, L201 (1977).

34. P.H. Kobrin, U. Becker, S. Southworth, C.M. Truesdale, D.W. Lindle, and D.A. Shirley, Phys. Rev. A 26, 842 (1982).

35. G.V. Marr and J.B. West, At. Data Nucl. Data Tables 18, 497 (1976).

36. U. Fano and J.W. Cooper, Phys. Rev. 137, A1364 (1965).

37. V.S. Senashenko and A. Wagué, J. Phys. B 12, L269 (1979).

38. U. Fano and J.W. Cooper, Rev. Mod. Phys. 40, 441 (1968).

39. P.G. Burke and D.D. McVicar, Proc. Phys. Soc. (London) 86, 989 (1965).

Table I. Total cross section and 1s partial cross section for He in the vicinity of the 3s3p resonance.

Photon energy (eV)	Total cross section (Mb)[a]	1s cross section (Mb)[a]
67.9	1.07(2)	0.983(13)
68.4	1.045(9)	0.951(9)
68.9	1.019(6)	0.932(6)
69.1	1.013(9)	0.925(9)
69.3	1.004(6)	0.919(6)
69.5	0.974(9)	0.900(9)
69.6	0.959(9)	0.898(9)
69.7	0.949(9)	0.896(9)
69.75	0.953(11)	0.908(9)
69.8	0.957(9)	0.923(9)
69.85	0.966(6)	0.938(6)
69.9	0.981(9)	0.953(9)
69.95	1.002(6)	0.955(6)
70.0	1.026(9)	0.947(9)
70.05	1.047(6)	0.938(6)
70.1	1.045(9)	0.925(9)
70.15	1.032(6)	0.913(6)
70.25	1.015(9)	0.900(9)
70.3	0.998(6)	0.878(6)
70.5	0.972(9)	0.866(9)
70.7	0.962(6)	0.859(6)
70.9	0.947(11)	0.851(11)

[a]Errors quoted represent statistical uncertainties only.

Table II. Fano parameters for the total cross section of helium for the 3s3p resonance. The background cross section σ_0 was taken to be 20.24–0.223E Mb, where E is the photon energy in eV. The numbers in parentheses represent statistical errors only.

	This work	Dhez and Ederer (Ref. 27)
q	1.30(5)	1.36(20)
ρ^2	0.057(5)	0.012(3)
σ_0(Mb)	0.989(30)	0.957(30)
Γ(eV)	0.178(12)[a]	0.132(14)
E_0(eV)	69.917(12)[a]	69.919(7)

[a]From Ref. 8.

Table III. Resonance parameters for the $He^+(n\ell\epsilon\ell')$ partial cross sections for the 3s3p doubly excited state. The parameters for the 1s cross section are from the fit shown in Fig. 2, where the background cross section was taken to be 20.27-0.230E Mb, where E is the photon energy in eV. Numbers in parentheses represent statistical errors only.

	Fano parameters			Starace parameters	
Channel	q	ρ^2	σ_0(Mb)[a]	C_1	C_2
$1s\epsilon p$	3.0(1)	0.012(4)	0.892(5)	1.10(4)	0.072(24)
$n=2$[b]	0.70(6)	0.89(8)	0.097(5)	0.55(2)	1.24(2)
$2s\epsilon p$			0.030(4)	0.35(11)	0.92(33)
$2p\epsilon s$			0.045(7)	0.65(10)	1.38(18)
$2p\epsilon d$			0.022(3)	0.65(10)	1.38(18)

[a]Errors quoted for the nonresonance cross sections represent only the uncertainty in the partitioning of the total cross section.
[b]From I (Ref. 11).

Table IV. α_μ parameters and partial linewidths for the 3s3p resonance.

Final state	$Re(\alpha_\mu)$	$Im(\alpha_\mu)$	$\lvert\alpha_\mu\rvert^2$	$(\Gamma_\mu/\Gamma)\times 100$
$1s\epsilon p$	0.000(15)	-0.036(19)	0.0013(10)	2.0(16)
n=2	0.67(5)	0.25(7)	0.57(6)	98(2)
$2s\epsilon p$	0.46(17)	0.13(28)	0.23(12)	12(7)
$2p\epsilon s$	0.76(9)	0.30(15)	0.72(14)	58(16)
$2p\epsilon d$	0.76(9)	0.30(15)	0.72(14)	28(7)

Table V. Matrix elements and oscillator strengths for the 3s3p resonance.

Matrix element	Magnitude: This work	Magnitude: Oscillator Strength
$\lvert\langle 3s3p\lvert\vec{r}\rvert 1s^2\rangle\rvert^2$	$1.3(2) \times 10^{-3}$ Mb [6.8×10^{-4} Mb][a]	$2.4(3) \times 10^{-4}$[b]
$\lvert\langle 1s\epsilon p\lvert\vec{r}\rvert 1s^2\rangle\rvert^2$	0.60(2) Mb/Ry	0.0081(3) eV^{-1}
$\lvert\langle 2s\epsilon p\lvert\vec{r}\rvert 1s^2\rangle\rvert^2$	0.020(3) Mb/Ry	0.00018(3) eV^{-1}
$\lvert\langle 2p\epsilon s\lvert\vec{r}\rvert 1s^2\rangle\rvert^2$	0.030(5) Mb/Ry	0.00027(5) eV^{-1}
$\lvert\langle 2p\epsilon d\lvert\vec{r}\rvert 1s^2\rangle\rvert^2$	0.015(2) Mb/Ry	0.00014(2) eV^{-1}
$\lvert\langle 3s3p\lvert V\rvert 1s\epsilon p\rangle\rvert^2$	$4.3(33) \times 10^{-5}$ Ry [2.8×10^{-5} Ry][a]	
$\lvert\langle 3s3p\lvert V\rvert 2s\epsilon p\rangle\rvert^2$	$2.5(14) \times 10^{-4}$ Ry	
$\lvert\langle 3s3p\lvert V\rvert 2p\epsilon s\rangle\rvert^2$	$1.2(3) \times 10^{-3}$ Ry	
$\lvert\langle 3s3p\lvert V\rvert 2p\epsilon d\rangle\rvert^2$	$5.9(15) \times 10^{-4}$ Ry	

[a]Fano and Cooper, Ref. 36.
[b]From Eq. 12.

Figure Captions

Fig. 1. Total cross section of He in the vicinity of the $1s^2 \rightarrow 3s3p$ resonance scaled to Marr and West (Ref. 35) at 68.9 eV. The solid curve is a fit to the data using the Fano formula [Eq. (2)] convoluted with a Gaussian function of 0.19 eV (0.48Å) FWHM to account for monochromator broadening. The corresponding Fano parameters are presented in Table II. The dashed curve is an absorption measurement from Ref. 27.

Fig. 2. He 1s partial cross section as in Fig. 1. The 1s Fano parameters are presented in Table III.

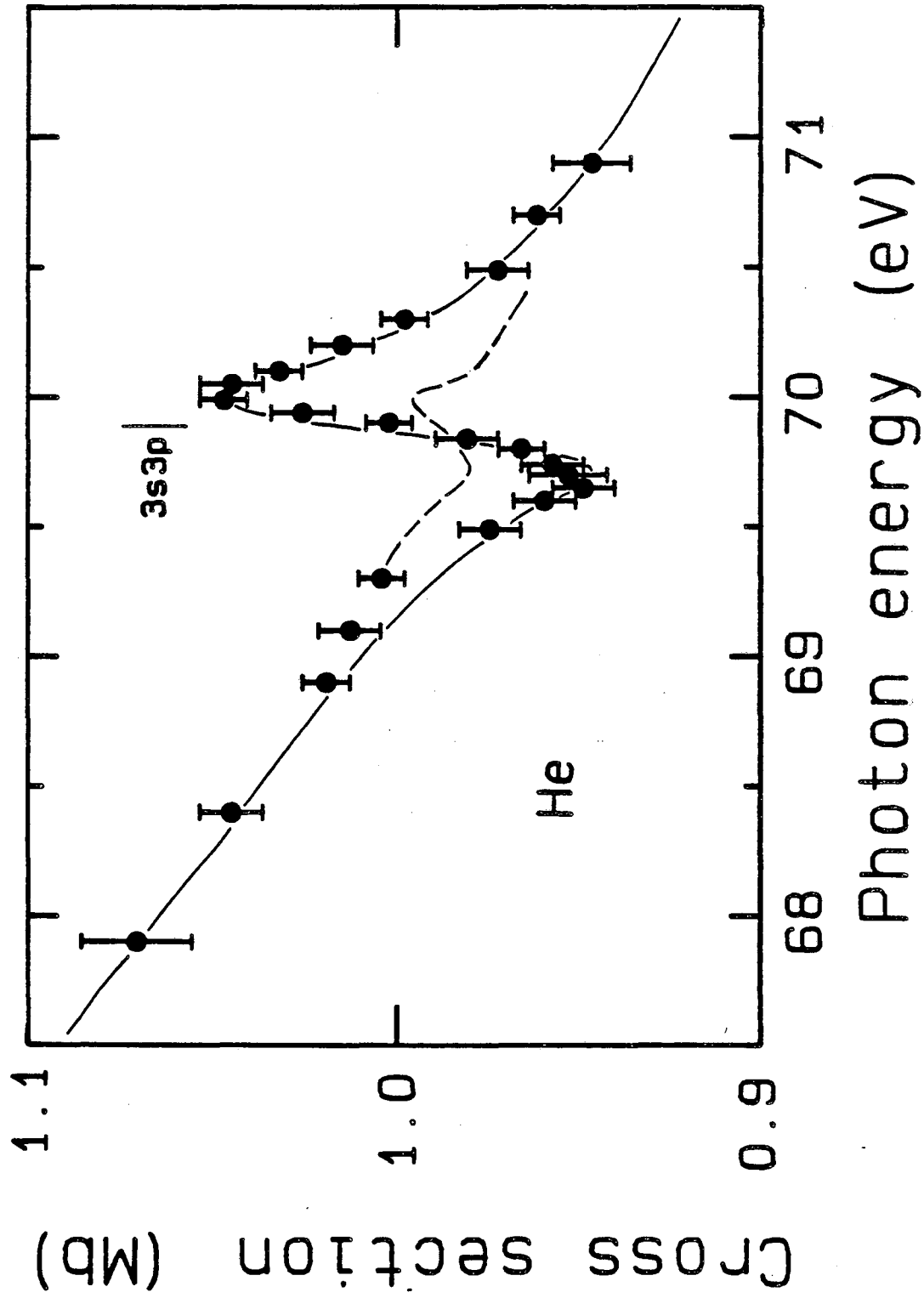

XBL 872-556

Figure 1

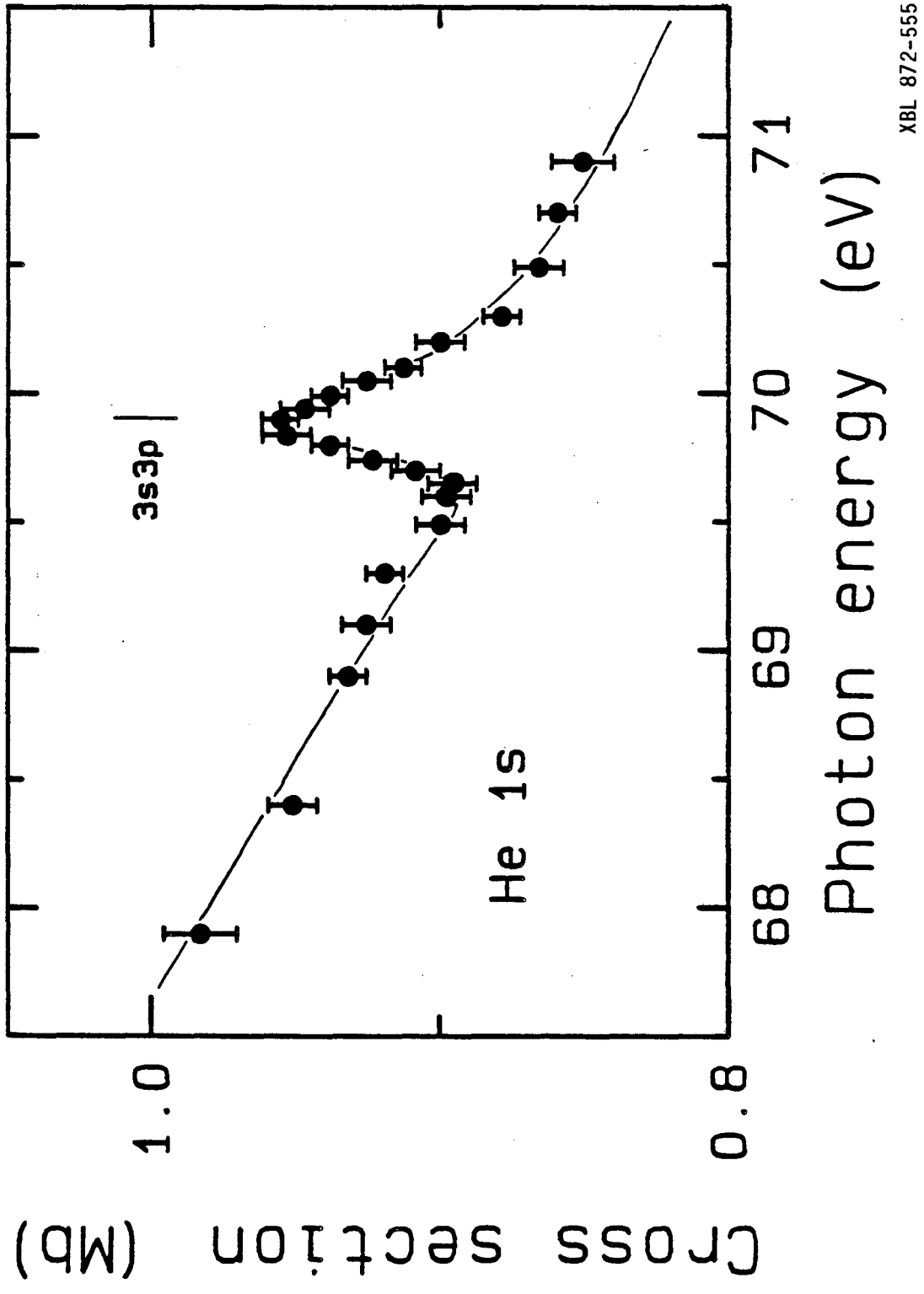

XBL 872-555

Figure 2

LAWRENCE BERKELEY LABORATORY
TECHNICAL INFORMATION DEPARTMENT
UNIVERSITY OF CALIFORNIA
BERKELEY, CALIFORNIA 94720